A TECHNIQUE FOR HIGH STRAIN RATE SHPB TESTING OF OFF-AXIS CARBON FIBER COMPOSITES

Qida Bing and C. T. Sun

School of Aeronautics and Astronautics, Purdue University, West Lafayette, IN, 47907-1282, USA

ABSTRACT

The present study aims at characterizing the strain rate dependent behaviour of polymer matrix composite (unidirectional AS4/3501-6) using off-axis composite specimens and the split Hopkinson pressure bar (SHPB). It was found experimentally in SHPB tests that strong interface friction existed for specimens of various off-axis angles resulting in bending waves in the bars and, thus, violating the assumptions of the SHPB analysis. In order to allow a fully developed extension–shear coupling in off-axis specimens under compression, titanium coating is applied through the use of the vapor deposition technique at the contact ends of the off-axis specimen. The titanium coating prevents the direct contact between the carbon fiber endings with the load applying contact surfaces and allows smooth sliding induced by the shear deformation. Stress-strain curves are generated at different strain rates using this type of specimen with strain controlled test. These curves are then used to develop a rate-dependent constitutive model which is used to predict rate-dependent compressive strength of the composite. Comparison of model predictions with experimental data indicates that the compressive strength model obtained by using low strain rate tests is valid for high strain rate also.

1. INTRODUCTION

Composites have been used more and more widely not only in traditional aerospace structures, but also in marine structures and armours which are subjected to dynamic loads. It is well known that the mechanical properties of polymer matrix composites are highly strain rate dependent; characterizing and modeling the dynamic constitutive behaviour and dynamic strength have attracted increasing interests from researchers.

Because of the anisotropic and nonlinear behaviour of polymer matrix composites, constitutive models for describing the rate dependent properties of these composites are not simple. Recently, Sun and co-authors [1-3] have developed a rather simple technique using off-axis composite specimens to generate stress-strain curves for different strain rates; from these curves a nonlinear rate-dependent model is obtained in terms of effective stress and effective plastic strain. However, this technique does not work for composite materials with high modulus fibers such as carbon fibers in compressive tests. Ninan et al [4] found that, in compression tests of off-axis specimens, endings of stiff fibers can make a significant indentation on the contact surface and restrain the shear deformation from taking place fully, leading to a nonuniform state of stress because of bending. By lapping the contact surfaces of the specimen and applying lubricant, Ninan et al [4] were able to essentially eliminate bending in glass/epoxy composites, but not in AS4/3501-6 carbon/epoxy composites because of the high stiffness of carbon fibers.

The purpose of the present work is to introduce a new technique to fully realize the extension-shear coupling in uniaxial compression tests. This technique involves placing Titanium coating on the contact surfaces of the off-axis specimen to prevent the direct contact of fiber endings and the loading surface. Low strain rate compression tests are performed on AS4/3501-6 carbon/epoxy composite using this type of specimen. The stress-strain curves obtained at various strain rates are then used to develop a rate-dependent compressive strength model following the procedure established by Tsai and Sun [3, 7]. This compressive strength model is used to predict the rate dependent microbuckling failure in off-axis specimens at high strain rates.

2. MATERIAL & SPECIMEN

Small block off-axis specimens with dimensions of 10x7x6mm were cut from a 48-ply unidirectional AS4/3501-6 laminate (AS4/3501-6: ply thickness is 0.127mm and fiber volume fraction is 0.65) by using a water-jet cutting machine (FLOW^{TM}). The fiber orientations considered included 5^{o}, 11^{o}, 15^{o}, 30^{o}, 45^{o} and 65^{o} with respect to the loading direction as shown in Fig. 1. In order to achieve a nearly frictionless contact between the specimen and the loading element, the ends of the specimen were polished with No.400, No.600 sand papers and lapped by using a lapping machine (HYPREZ^{TM}) with 15μm, 6μm diamond slurries first. Subsequently, a 1.2μm (based on the surface average roughness measured) titanium layer was added on both end surfaces with a Leybold E-Beam Evaporator. The micrographs in Fig. 2 shows that the fiber ends were covered totally by the titanium coating.

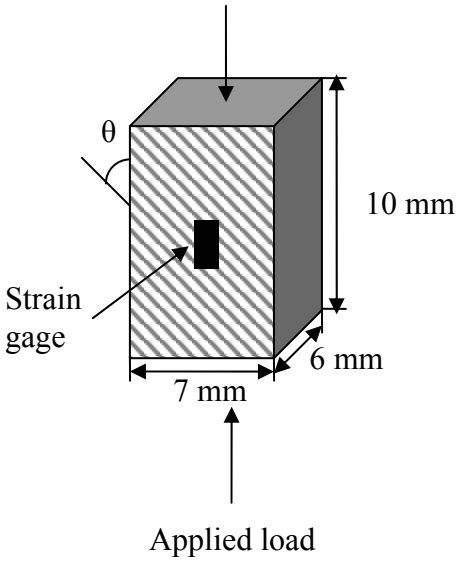

"**Fig. 1.** Small brick off-axis specimen with off-axis angle θ."

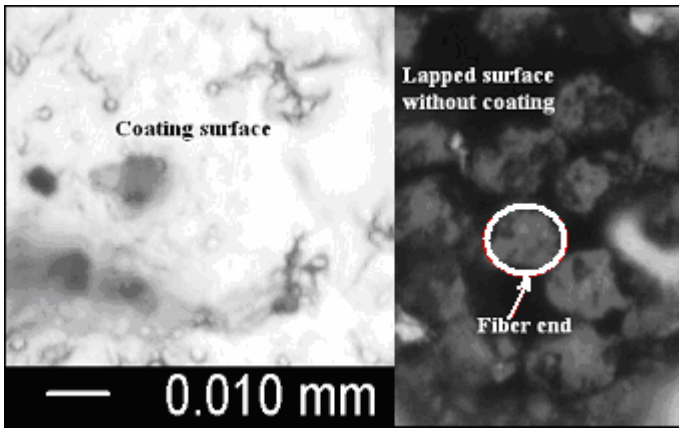

"**Fig. 2.** Micrographs showing fiber ends in specimens with coating and without coating

3. HIGH STRAIN RATE TEST

Split Hopkinson Pressure Bar (SHPB) is a simple but rather accurate way for high strain rate testing of materials [5-6]. As shown in Fig. 3, the SHPB system consists of basically the striker bar, the incident bar, and the transmission bar. The strain in the incident and transmission bars must be uniaxial. This requires that the reaction from the specimen be only a pressure. This condition would be violated if a shearing force is produced from the shear

deformation in the off-axis specimen in the presence of contact friction. This frictional shearing force would give rise to transverse deflections (bending wave) in both the incident and transmission bars. To detect if such a bending wave is induced during the test, two strain gages were mounted at location C (Fig. 3) in the transmission bar. The magnitude of the induced bending strain at location C indicates the amount of friction generated at the contact surfaces.

The SHPB setup consists of A2 hardened steel bars of 12.7mm in diameter. The strike bar is 152mm long, the incident bar is 914mm long and the transmission bar is 559mm long. A pair of strain gauges is mounted at the mid-span of the incident bar, and another pair is mounted on the transmission bar at 178mm from the specimen – bar interface. The pair of strain gages at location C for detecting bending waves is about 25mm from the end of the transmission bar. The strain gages to pick up bending waves are connected to a Wheatstone bridge circuit in a ½ bridge way to nullify axial waves and magnify two times to the bending waves. The signals from the bridges are amplified 500 times by AM 502 Differential amplifiers, recorded in a Tektronix TDS400 oscilloscope and later acquired by a PC for subsequent analysis. The data sampling rate is 10MHz for all SHPB tests in the present work.

Strain signals for the 15^{o} AS4/3501-6 off-axis specimens with different end treatments were recorded at gages at locations A, C, and D and are shown in Figs. 4-6. The result clearly indicates that lapped and lubricated specimens can remarkably reduce the bending effect, but cannot eliminate it. For the specimen coated with titanium, bending is negligible and uniaxial loading is assured.

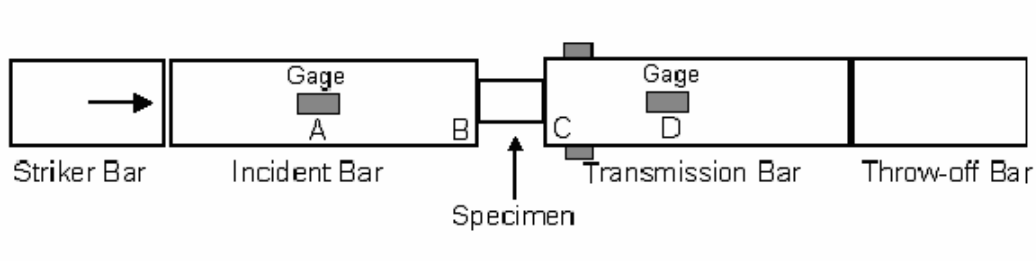

"**Fig. 3.** Schematic of Split Hopkinson Pressure Bar."

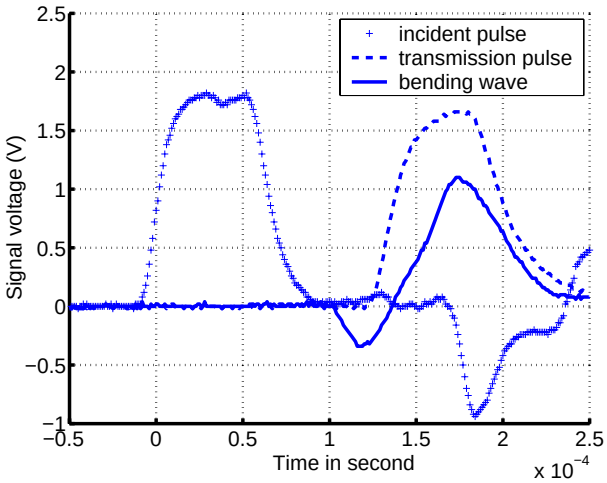

"**Fig. 4.** Strain histories picked up by strain gages at locations A, C, and D in lapped 15^{o} off-axis AS4/3501-6 composite specimen w/o lubricant."

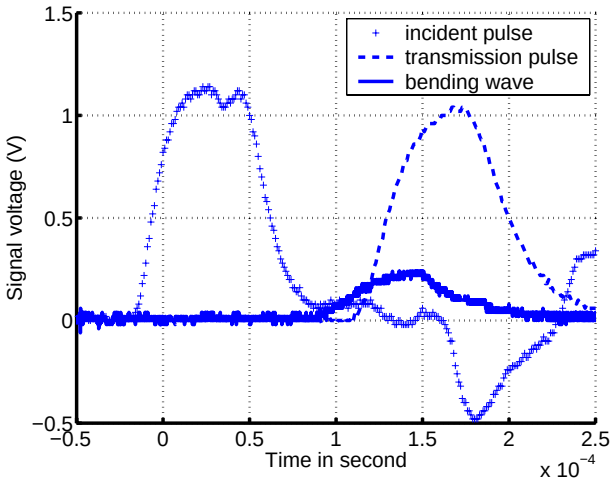

"**Fig. 5.** Strain histories picked up by strain gages at locations A, C, and D in lapped 15° off-axis AS4/3501-6 composite specimen with lubricant."

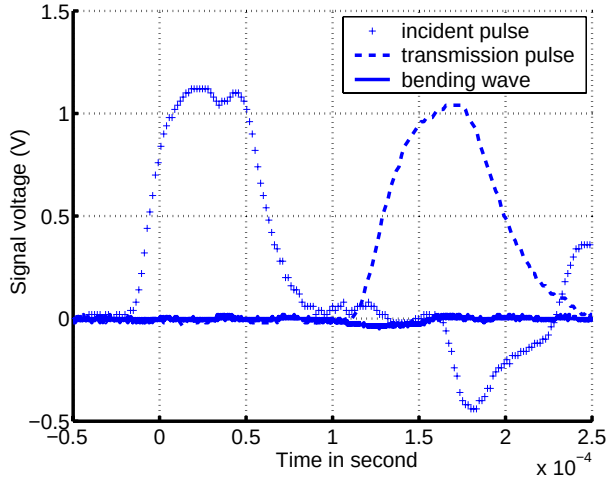

"**Fig. 6.** Strain histories picked up by strain gages at locations A, C, and D in 15° off-axis AS4/3501-6 composite specimen coated with titanium and tested with lubricant."

4. TESTING COMPRESSIVE STRENGTH

To study the coating effect on microbuckling compressive strength which means the microbuckling failure is the specimen failure mode, off-axis AS4/3401-6 composite specimens with and without end coating were tested in compression at strain rates of 10^{-5}/s, 10^{-3}/s and 10^{-1}/s using an MTS machine in strain controlled test mode and at 400 - 700/s on a SHPB. The strain rate in the SHPB test was estimated using the Hopkinson bar formula and was not very accurate. However, for the present purpose, the estimated strain rate is adequate. In both types of specimens, lubricant was used. In uniaxial compression tests performed on the MTS machine, a self-adjusting device was used in order to ensure the specimen to be in full contact with the loading element and eliminate potential bending moments as shown in Fig. 7. Table 1 lists the average compressive strengths for both types of specimens.

It is noted that the compressive strengths of coated off-axis specimens at low strain rates (10^{-5}/s, 10^{-3}/s and 10^{-1}/s) are lower than those of uncoated specimens. However at high strain rates in SHPB tests in which the range of strain rate was about 400~700/s, the strengths of coated off-axis specimens are greater than those of uncoated specimens. The reason is that at low strain rate loading there is a higher level shear stress in the coated specimen, which can cause

a reduction in compressive strength in the fiber composite [7]. However in the high strain rate SHPB test, the shear stiffness of the epoxy matrix of coated specimen increases significantly. Since microbuckling strength is proportional to the elastic-plastic shear modulus of the composite [7], this explains why the coated specimen has a higher compressive strength than the uncoated one at high strain rates.

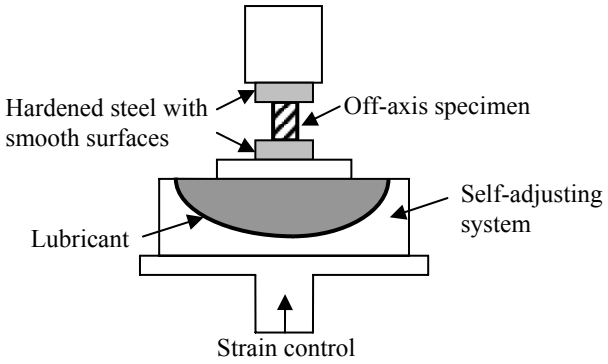

"**Fig. 7.** Schematic of compression test with self-adjusting system."

"**Table 1.** Strength comparison between lapped and coated samples."

Strain rate	Off-axis angle	Strength (MPa)		Decrease	Increase
		Uncoated sample	Coated sample		
10^{-5}/s	5	721.8	649.7	10.0%	
	11	433.7	420.9	3.0%	
	15	352.3	331.7	5.8%	
10^{-3}/s	5	734.8	729.4	0.7%	
	11	471.2	460.9	2.2%	
	15	384.1	366.4	4.6%	
10^{-1}/s	5	849.7	837.7	1.4%	
	11	537.0	487.0	9.3%	
400~700/s	5	990.1	1031.3		4.2%
	11	618.3	660.8		6.9%

5. COATING EFFECT ON FAILURE MODES

Two failure modes were observed for both coated and uncoated off-axis specimens depending on off-axis angles and strain rates. Fiber microbuckling failure (compression failure) was observed in both coated and uncoated specimens with 5^o and 11^o off-axis angles for all strain rates considered. Matrix shear failure mode was found for both types of specimens with off-axis angles greater than 15^o. For 15^o off-axis specimens, microbuckling failure was observed when the applied strain rate was 10^{-5}/s (Fig. 8), and matrix shear failure occurred when strain rates were beyond 10^{-1}/s (see Fig. 9). At the strain rate of 10^{-3}/s, there is a difference between the failure modes in the coated and uncoated specimens. At this strain rate, the coated specimen failed in matrix shearing failure mode while the uncoated specimen failed in fiber microbuckling mode.

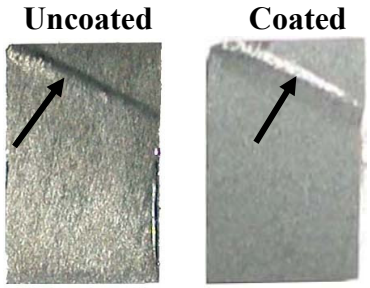

"**Fig. 8.** Microbuckling failure mode in 15° coated and uncoated specimens at 10^{-5}/s strain rate."

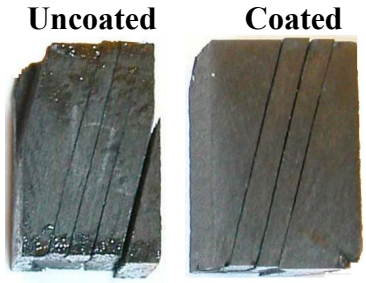

"**Fig. 9.** Matrix shear failure for 15° coated and uncoated specimens at strain rates higher than 10^{-1}/s."

6. COMPRESSIVE STRENGTH PREDICTION

The compression failure model developed by Sun and coauthors [1-3, 8] is adopted in this study. First, off-axis composite specimens with coating are used to generate stress-strain curves at different strain rates. From these stress-strain curves a rate-dependent nonlinear constitutive model is developed. The constitutive model is given by

$$\dot{\bar{\varepsilon}}^p = A(\bar{\sigma})^n \tag{1}$$

where $\bar{\sigma}$ is effective stress, $\dot{\bar{\varepsilon}}^p$ is the corresponding effective plastic strain rate [2-3]. The effective stress is defined as

$$\bar{\sigma} = \sqrt{3f} \tag{2}$$

where

$$f = \frac{1}{2}[(\sigma_{22} - \sigma_{33})^2 + 4\sigma_{23}^2 + 2a_{66}(\sigma_{12}^2 - \sigma_{13}^2)] \tag{3}$$

is a 3-D plastic potential for transversely isotropic composites [8]. Note that in Eq. (1), A is a function of effective plastic strain rate and can be assumed to be in the form of the power law, i.e.,

$$A = \chi(\dot{\bar{\varepsilon}}^p)^m \tag{4}$$

A complete 3-D model can be derived based on the low strain rate data obtained from the MTS strain controlled testing of off-axis composite specimens.

The stress-strain curves for AS4/3401-6 carbon/epoxy composite obtained at various strain rates using strain controlled tests are shown in Figs. 10-12. These strain rate-dependent stress-strain curves are used to develop the constitutive model. Following the procedure established by Tsai and Sun [3], these off-axis curves for each strain rate can be collapsed into a single

master curve in terms of effective stress and effective plastic strain as shown in Figs. 13-15. These master curves are fitted with a power law as shown in Fig. 16. The results in Fig. 16 are used to determine A as a function of effective plastic strain rate which is presented on the log-log scale in Fig. 17. Table 2 lists the values of the parameters in the constitutive model for AS4/3501-6 carbon/epoxy composite.

The compressive strength of an off-axis composite is given by

$$\sigma_{xc}\cos^2(\theta+\theta_{mis}+\gamma_{12})=\left[\frac{1}{G_{12}^e}+\frac{6a_{66}^2\cos^2(\theta+\theta_{mis}+\gamma_{12})}{H_p[\sin^2(\theta+\theta_{mis}+\gamma_{12})+2a_{66}\cos^2(\theta+\theta_{mis}+\gamma_{12})]}\right]^{-1} \tag{5}$$

where σ_{xc} is composite off-axis compressive strength, θ is off-axis angle, θ_{mis} is initial fiber misalignment angle, γ_{12} is in-plane shear strain, G_{12}^e is elastic shear modulus of the composite and H_p is plastic modulus of the composite. Details of this model can be found in [7]. For a given off-axis angle θ and load history, a numerical iteration is employed to obtain the microbuckling strength σ_{xc}. As time increases incrementally from zero, at each time step, the uniaxial stress σ_x, the effective stress $\bar{\sigma}$, the current strain ε and the plastic modulus H_p are calculated using the constitutive model [8], the current in-plane shear strain is also obtained by adding all the previous shear strain increments. The applied stress is the microbuckling strength σ_{xc} when Eq. (5) is satisfied. This model, although established with data obtained at strain rates below 1/s, can be used to predict compressive strengths for high strain rates. Table 3 lists the predictions with 2.5° initial fiber misalignment [9]. It is noted that the predictions and test results agree very well even for the data obtained from the SHPB test at a strain rate of 250/s.

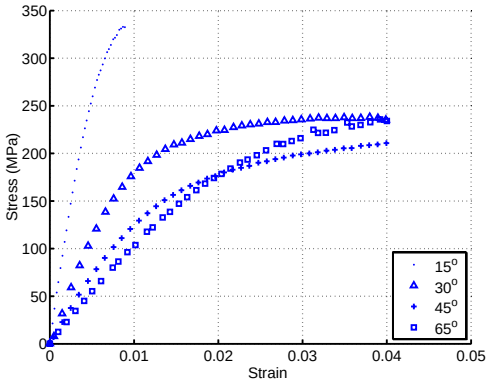

"**Fig. 10.** Stress-strain curves at 10^{-5}/s strain rate."

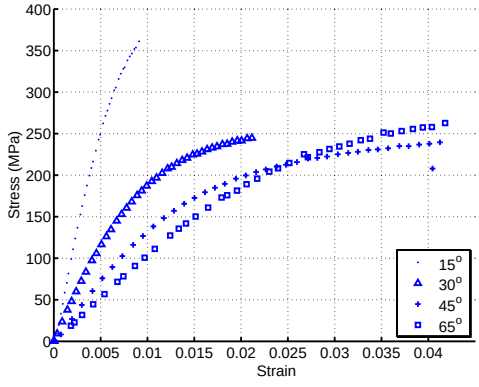

"**Fig. 11.** Stress strain curves at 10^{-3}/s strain rate."

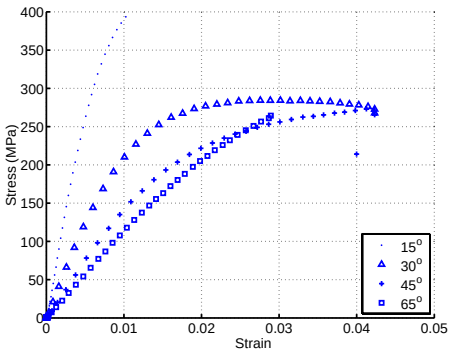

"**Fig. 12.** Stress strain curves at 10^{-1}/s strain rate."

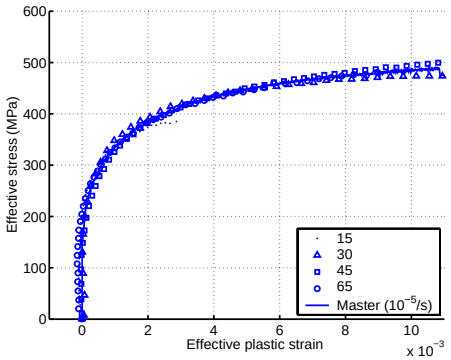

"**Fig. 13.** Collapsed effective stress – effective plastic strain curves for AS4/3501-6 carbon fiber composite at strain rate 10^{-5}/s with a_{66}=7.0."

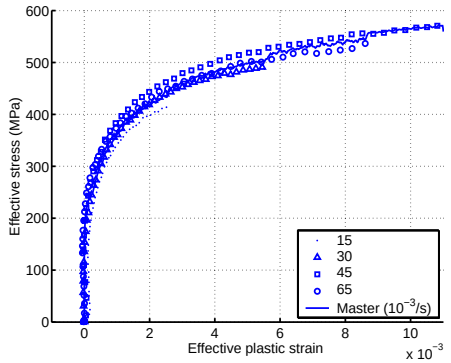

"**Fig. 14.** Collapsed effective stress – effective plastic strain curves for AS4/3501-6 carbon fiber composite at strain rate 10^{-3}/s with a_{66}=7.0."

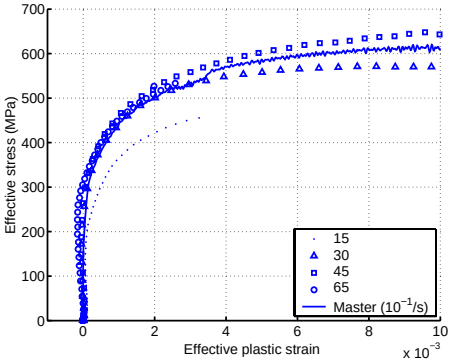

"**Fig. 15.** Collapsed effective stress – effective plastic strain curves for AS4/3501-6 carbon fiber composite at strain rate 10^{-1}/s with a_{66}=7.0."

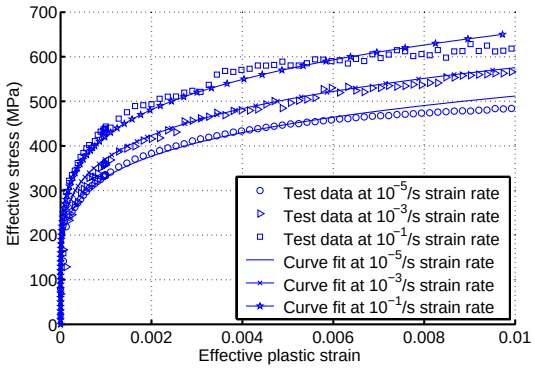

"**Fig. 16.** Effective stress – effective plastic strain curves at various strain rates."

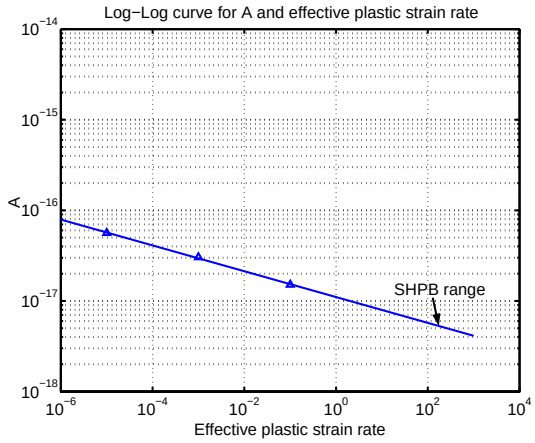

"**Fig. 17.** Log-log plot for the rate-dependent amplitude A."

"**Table 2.** Parameters for the viscoplasticity model for AS4/3501-6 carbon/epoxy composite."

Viscoplasticity model parameters	Value
a_{66}	7.0
χ	1.1E-17$(MPa)^{-n}$
m	-0.1425
n	5.26

"**Table 3.** Model predictions and test results for compressive strengths."

Strain rate	Off-axis angle (^{o})	Test result (MPa)	Model prediction (MPa)
10^{-5}/s	5	649.7	627
	11	420.9	419
	15	331.7	355
10^{-3}/s	5	729.4	706
	11	460.9	472
	15	366.4	401
10^{-1}/s	5	837.7	801
	11	487.0	530
250/s	5	934.9	951
	11	597.2	632

7. LONGITUDINAL COMPRESSIVE STRENGTH

Testing 0^o composite specimens for their compressive strengths is not an easy task. Instead of microbuckling failure, other failure modes such as end brooming or fiber splitting often occur first. The microbuckling model can be used to predict longitudinal compressive strength of the composite. With a fiber misalignment angle of 2.5^o, the model predicts the longitudinal compressive strengths of the AS4/3501-6 composite for different strain rates as listed in Table 4.

"**Table 4.** Predicted longitudinal compressive strength for AS4/3501-6 carbon/epoxy composite."

Strain rate (1/s)	Compressive strength (MPa)
10^{-5}	1390
10^{-3}	1547
10^{-1}	1715
250	2034

8. CONCLUSIONS

A new technique using titanium coating on the contact surfaces of off-axis composite specimens was employed to characterize the strain rate dependent behaviour of carbon fiber composites. It was found that titanium coating can eliminate the specimen/loading surface interfacial friction in compression tests and allow extension-shear coupling to be fully developed. The effects of titanium coating on compressive strength and failure mode at various strain rates were studied. Based on the microbuckling model and the rate-dependent constitutive model for the composite, the predicted compressive strengths for off-axis specimens agree very well with the test data. It can be also concluded that the compressive strength model developed with low strain rate test data can be used to predict compressive strengths at high strain rates.

ACKNOWLEDGEMENTS

This work was supported by an Office of Naval Research Grant No. N00014-96-0822. Dr. Yapa D. S. Rajapakse was the program manager.

References

1. **Weeks, C.A.** and **Sun**, **C.T.**, "Modeling Nonlinear Rate Dependent Behavior in Fiber Reinforced Composites", *Compos Sci Technol.*, **58** (1998), 603-611.
2. **Thiruppukuzhi, S.V.** and **Sun, C.T.**, "Models for Strain Rate-Dependent Behavior of Polymer Composites", *Compos Sci Technol.,* **61** (2001), 1-12.
3. **Tsai, J.** and **Sun, C.T.**, "Constitutive Model for High Strain Rate Response of Polymeric Composites", *Compos Sci Technol.,* **62** (2002), 1289-1297.
4. **Lal Ninan**, **Tsai, J.**, and **Sun C.T.**, "Use of Split Hopkinson Pressure Bar for Testing Off-axis Composites", *Int. J. Impact Eng.*, **25** (2001), 291-313.
5. **Davies, E.D.H.** and **Hunter, S.C.**, "The dynamic compression testing of solids by the method of the split Hopkinson pressure bar", *J. Mech Phys Solids*, **11** (1963), 155-179.
6. **Follansbee, P.S.** and **Frantz, C.,** "Wave propagation in the split Hopkinson pressure bar", *J Eng Mater Technol.*, 105 (1983), *J Eng Mater Tech.*, **105** (1983), 61-66.
7. **Tsai, Jialin** and **Sun, C.T.**, "Dynamic Compressive Strengths of Polymeric Composites", to be published in *Int J Solids and Structures.*
8. **Sun, C.T.** and **Jun, A. Wanki,** "Compressive strength of unidirectional fiber composites with matrix non-linearity", *Compos Sci Technol.*, **52** (1994), 577-587
9. **Thiruppukuzhi, S.V.** and **Sun, C.T.**, "Testing and modelling high strain rate behaviour of polymeric composites", *Composites Part B,* **29B** (1998), 535-546